AIAA JOURNAL
Vol. 36, No. 10, October 1998

Further Development of the k–ζ (Enstrophy) Turbulence Closure Model

D. F. Robinson* and H. A. Hassan†
North Carolina State University, Raleigh, North Carolina 27695-7910

The k–ζ model is extended to the study of two-dimensional and three-dimensional separated external flows where Morkovin's hypothesis is expected to hold. The resulting model is free of damping and wall functions and is coordinate independent. Further, all modeled correlations are tensorially consistent and Galilean invariant. Applications include a variety of separated flows over airfoils and a cylinder/offset flare juncture. Comparisons are made with other turbulence models and experiment. In general, good agreement with experiment is indicated. The results demonstrate that it is possible to develop a two-equation turbulence model that is capable of predicting separated flows without sacrificing performance for free shear layers.

Introduction

DIFFICULTIES encountered in the calculation of turbulent shear flows can be traced to the high turbulent Reynolds numbers hypotheses, where the large scales are unaffected by the fluid's viscosity and where the small scales are unaffected by the mean flow or the large scales. Thus, traditional two-equation models, such as the k–ε and k–ω models and a variety of stress models, cannot predict all growth rates of free shear flows using one set of model constants and boundary conditions.[1] Additional problems are encountered when one considers flows in the presence of adverse pressure gradients and flow separation, especially shock-induced separation.

Morse[2] pointed out that some of the problems were a result of an inadequate dissipation rate equation. In spite of this, the thrust of research in the last 20 years has been devoted to stress models or second-order closure. This strategy proved to be unsatisfactory for free and wall-bounded shear flows. This is to be expected; if the dissipation rate equation is incorrect, then a stress model cannot yield correct answers irrespective of the level of sophistication used in modeling the pressure–strain term.

The fine-scale correlations that appear in the dissipation rate equation are the ones that describe the detailed mechanism of the dissipation process and, thus, control the behavior near turbulent/nonturbulent interfaces. Thus, if we hope to accurately calculate skin friction, heat transfer, and growth rates of free shear layers, then the fine-scale correlations must be modeled and included in modeled equations. This was the primary motivation for Robinson et al.[3] to undertake the development of the k–ζ model.

In general, and depending on the nature of the flow under consideration, there are different mathematically consistent ways of expressing a correlation. As an illustration, for low-speed constant pressure flows, correlations can be expressed in terms of velocity gradients k and ζ and their derivatives. Compressible flows introduce two thermodynamic variables, and their influence must be reflected in evaluating correlations. Thus, modeling a correlation for complex flows is a tedious and time-consuming undertaking.

The k–ζ model was used in the study of free and wall-bounded shear flows for both low- and high-speed flows.[3–7] In general, the predictions of the model were as good or better than k–ε or k–ω models. This is especially true for free shear flows and separated flows. Many improvements in the basic k–ε and k–ω models have been made.[1] However, none of these improvements resulted in a model that was capable of predicting adverse pressure gradient flows without sacrificing performance of free shear layers. These results clearly illustrate the importance of using a more accurate dissipation rate equation.

Various forms of the k–ζ model were used in various conference papers[4–7] that dealt with two-dimensional flows. The goal of this work is to present the final version of the model and to demonstrate it for two- and three-dimensional separated flows. As will be seen, the model is free of damping and wall functions and is coordinate invariant. Further, all modeled correlations are tensorially consistent and Galilean invariant.

Problem Formulation

The exact Favre-averaged compressible turbulence kinetic energy and enstrophy equations can be written as

$$\frac{\partial}{\partial t}(\bar\rho k)+\frac{\partial}{\partial x_j}(\bar\rho\tilde u_j k)=\tau_{ij}\frac{\partial\tilde u_i}{\partial x_i}-\bar\rho\varepsilon-\overline{u_i''}\frac{\partial\bar P}{\partial x_i}+\overline{p'\frac{\partial u_i''}{\partial x_i}}+\frac{\partial}{\partial x_j}\left(\overline{t_{ji}u_i''}-\overline{\frac{\rho u_j''u_i''u_i''}{2}}-\overline{p'u_j''}\right) \tag{1}$$

$$\begin{aligned}&\frac{\partial}{\partial t}\left(\bar\rho\widetilde{\omega_i''^2}\right)+\frac{\partial}{\partial x_k}\left(\bar\rho\tilde u_k\widetilde{\omega_i''^2}+2\Omega_i\overline{\rho u_k''\omega_i''}+\overline{\rho u_k''\omega_i''^2}\right)\\&\quad-2\Omega_i\frac{\partial}{\partial x_k}\left(\overline{\rho u_k''\omega_i''}\right)=2\left(\Omega_m\overline{\rho\omega_i''s_{im}''}+\tilde s_{im}\overline{\rho\omega_i'\omega_m''}\right.\\&\quad\left.+\overline{\rho\omega_i''\omega_m''s_{im}''}-\bar\rho\tilde s_{kk}\widetilde{\omega_i''^2}-\Omega_i\overline{\rho\omega_i''s_{kk}''}-\overline{\rho s_{kk}''\omega_i''^2}\right)\\&\quad+2\frac{\varepsilon_{ijk}}{\bar\rho}\left[\overline{\frac{\partial\bar\rho}{\partial x_j}\omega_i'\left(\frac{\partial p'}{\partial x_k}-\frac{\partial t_{km}'}{\partial x_m}\right)}+\overline{\omega_i'\frac{\partial\rho'}{\partial x_j}}\left(\frac{\partial\bar P}{\partial x_k}-\frac{\partial\bar t_{km}}{\partial x_m}\right)\right.\\&\quad\left.+\overline{\omega_i'\frac{\partial\rho'}{\partial x_j}\left(\frac{\partial p'}{\partial x_k}-\frac{\partial t_{km}'}{\partial x_m}\right)}+\bar\rho\overline{\omega_i'\frac{\partial^2 t_{km}'}{\partial x_j\partial x_m}}\right]\end{aligned} \tag{2}$$

where

$$s_{ij}''=\frac{1}{2}\left(\frac{\partial u_i''}{\partial x_j}+\frac{\partial u_j''}{\partial x_i}\right),\qquad \tilde s_{ij}=\frac{1}{2}\left(\frac{\partial\tilde u_i}{\partial x_j}+\frac{\partial\tilde u_j}{\partial x_i}\right)$$

$$\Omega_i=\varepsilon_{ijk}\frac{\partial\tilde u_k}{\partial x_j},\qquad \omega_i''=\varepsilon_{ijk}\frac{\partial u_k''}{\partial x_j},\qquad k=\frac{\widetilde{u_i''u_i''}}{2}$$

$$\zeta=\widetilde{\omega_i''\omega_i''},\qquad \tau_{ij}=\bar\rho\widetilde{u_i''u_j''},\qquad t_{ij}=2\mu s_{ij}-\frac{2}{3}\mu\frac{\partial u_k}{\partial x_k}\delta_{ij}$$

$$u_i=\tilde u_i+u_i''=\bar u_i+u_i',\qquad \nu=\frac{\mu}{\rho} \tag{3}$$

Received Nov. 30, 1997; revision received May 30, 1998; accepted for publication June 12, 1998.

*Research Assistant, Mechanical and Aerospace Engineering; currently Aerospace Engineer, Code G72, U.S. Naval Surface Warfare Center, Dahlgren Division, Dahlgren, VA 22448-5100. Student Member AIAA.

†Professor, Mechanical and Aerospace Engineering. Associate Fellow AIAA.

and ρ is the density, μ is the viscosity, u_i is the velocity, P is the pressure, and ε is the rate of turbulent energy dissipation. Also, δ_{ij} and ε_{ijk} are the Kronecker delta and permutation tensor, respectively.

The low-speed equations were modeled in Ref. 3, which addressed low-speed free shear layers where the pressure is constant. Modifications presented here address the contributions of compressibility and pressure gradients. The modification is such that, if the effects of compressibility and pressure gradient are negligible, then one recovers the equation of Ref. 3.

Compressible flows require for their description a velocity field and two thermodynamic variables. Because of this, the fluctuations of these thermodynamic variables are as important as those of velocity in describing turbulent flows at high Mach numbers. Therefore, an appropriate compressible turbulent flow model of the two-equation variety should include six equations that describe variances of velocity, density, and temperature together with their respective dissipation rates. A simplification of this approach can be achieved by invoking Morkovin's hypothesis.[8] According to this hypothesis, the pressure and total temperature T_0 fluctuations are small for non-hypersonic boundary layers with conventional rates of heat transfer, i.e.,

$$p'/P \ll 1, \qquad T_0'/T_0 \ll 1 \tag{4}$$

As a result,

$$(\rho'/\rho) \simeq -(T'/T) \simeq (\gamma - 1)M^2(u'/u) \tag{5}$$

Based on this, equations governing variances of the thermodynamic variable can be taken as the equations governing the turbulence kinetic energy. However, equations governing their dissipation rates may be different from equations governing ε or ζ.

Modeling Issues

Modification of the k Equation

The dissipation rate in Eq. (1) is defined as[1]

$$\bar{\rho}\varepsilon = \nu\left[\overline{\rho\omega_i''\omega_i''} + 2\overline{\rho u_{i,j}'' u_{j,i}''} - \frac{2}{3}\overline{\rho(u_{i,i}'')^2}\right]$$

$$= \nu\left[\overline{\rho(\omega_i'')^2} + \frac{4}{3}\overline{\rho(u_{i,i}'')^2}\right] + 2\bar{\nu}\frac{\partial}{\partial x_i}[\overline{(\rho u_i'' u_j'')_{,j}} - \overline{2\rho u_i'' u_{j,j}''}] \tag{6}$$

Equation (6) assumes that correlations between velocity gradient and kinematic viscosity fluctuations are negligible. The second term in Eq. (6), i.e., $2\nu(\partial/\partial x_i)[\,]$, is either neglected or added to the diffusion term. The latter choice is made here.

The term $\frac{4}{3}\nu\rho(u_{i,i}'')^2$ is modeled as

$$\frac{c_1\bar{\rho}k}{\tau_\rho} \tag{7}$$

where c_1 is a model constant and τ_ρ is a timescale. Because the correlation under consideration is zero when the density is constant, τ_ρ is taken as

$$\frac{1}{\tau_\rho} = \left[\left(\frac{\partial\bar{\rho}}{\partial x_i}\right)^2 k\right]^{\frac{1}{2}} \Big/ \bar{\rho} \tag{8}$$

The Favre-averaged velocity fluctuation $\overline{u_i''}$ is traditionally modeled using a gradient diffusion assumption. Thus,

$$\overline{u_i''} = -\frac{\overline{\rho' u_i'}}{\bar{\rho}} = \nu_t\left(\frac{\partial\bar{\rho}}{\partial x_i}\right)\Big/ C_k\bar{\rho} \tag{9}$$

where c_k is a model constant and ν_t is the eddy viscosity

$$\nu_t = c_\mu k^2/\nu\zeta, \qquad c_\mu = 0.09 \tag{10}$$

Modifications of the ζ Equation

There are a number of compressibility terms in the ζ equation. The only term retained is $\bar{\rho}\overline{\omega_i'' s_{ij}''}\Omega_i$, which is a production term resulting from dilatational effects. The term is modeled as

$$C_{\zeta 1}(\mu_t/k)(\zeta/\tau_\rho)\Omega, \qquad \Omega^2 = \Omega_i\Omega_i \tag{11}$$

where $C_{\zeta 1}$ is a model constant.

The next modification addresses near-wall behavior. The dissipation term in the ζ equation was modeled in Ref. 3 as

$$\frac{\beta_5\zeta^{\frac{3}{2}}}{R_k}, \qquad R_k = R_t^{\frac{1}{2}}, \qquad R_t = \frac{k^2}{\nu^2\zeta} \tag{12}$$

To accommodate the requirement that turbulence timescale $k/\nu\zeta$ cannot be less than Kolmogorov's timescale, the dissipation term was modified to

$$\frac{\beta_5\zeta^{\frac{3}{2}}}{R_k + \delta} \tag{13}$$

where δ is chosen equal to 0.1. Another modification pertains to the value of σ_R that results from modeling the term $\overline{u_i''\omega_i''}$. The constant was selected in Ref. 3 based on considerations relevant to the log-law region. This is inappropriate. It is shown in Ref. 7 that the term $\overline{\rho u_i''\omega_i''}(\partial\Omega_i/\partial x_j)$, which is neglected in traditional turbulence models, plays a major role in eliminating damping functions. In particular, a value of σ_r of 0.07 makes it possible to remove f_μ from the definition of an eddy viscosity.

The need for introducing explicit dependence on the pressure gradient in the ζ equation was discussed in Ref. 6. The term used in Ref. 6 has the effect of increasing ζ and, thus, reducing eddy viscosity throughout the flowfield irrespective of whether the pressure gradient is favorable. The term used in Ref. 7 affected only the adverse pressure gradient region; however, it was not Galilean invariant. In the present work, the term is taken as $\max(P_\zeta, 0.0)$, where

$$P_\zeta = \frac{(\rho k\Omega/\nu\bar{P}\sigma_P)}{1 + (\sigma_\rho/\tau_\rho)(R_t/\zeta)^{\frac{1}{2}}}\frac{\mathrm{D}\bar{P}}{\mathrm{D}t} \tag{14}$$

where σ_P and σ_ρ are model constants. In the applications considered so far, P was calculated from the equation of state of a perfect gas. For liquids, where the static pressure may be determined only to within an arbitrary constant, P may be replaced by $\bar{\rho}a^2$, where a is the speed of sound. Because

$$\frac{1}{\bar{\rho}a^2}\frac{\mathrm{D}P}{\mathrm{D}t} \simeq M^2\frac{\mathrm{d}V}{\mathrm{d}s}$$

where M is the Mach number, V is the resultant speed, and s is the distance along a streamline, P_ζ is essentially negligible at extremely low Mach numbers.

The β_8 term had originally an Ω^2 in the denominator in Ref. 3. The term was replaced by $s^2 = \tilde{s}_{ij}\tilde{s}_{ij}$ in Refs. 6 and 7. In the present work, the denominator is taken as $s^2 + \Omega^2/2$. This adjustment removes potential difficulties in flows characterized by rigid-body rotation and in regions where the flow may be irrotational. Finally, the value of β_7 reported in Ref. 3 is in error; it should be 1.5.

A summary of the modeled equations is given in the Appendix, and the model constants are given in Table 1.

Table 1 k–ζ Model closure coefficients

Constant	Value
c_μ	0.09
κ	0.40
α_3	0.35
β_4	0.42
β_5	2.37
β_6	0.10
β_7	1.50
β_8	2.3
σ_r	0.07
σ_p	0.13
σ_ρ	91.90
$1/\sigma_k$	1.80
$1/\sigma_\zeta$	1.46
δ	0.10
C_1	0.60
C_k	2.00
$C_{\zeta 1}$	2.10

Boundary Conditions

The boundary conditions for the two-equation model are

$$k_w = 0, \qquad k_\infty = \tfrac{3}{2}(TuU_\infty)^2 \tag{15}$$

and

$$\left(\frac{\partial k}{\partial n}\right)_w = 0 \tag{16}$$

where Tu is the turbulent intensity, n is the direction of the normal to the surface, and subscripts w and ∞ designate the wall and freestream, respectfully. Here, ζ_∞ is determined from specifying $(\nu_t/\nu)_\infty$ (less than 10^{-2}) and k_∞, and ζ_w is determined from Eq. (16) and the modeled k equation as

$$(\mu\zeta)_w = \frac{1}{3}\frac{\partial}{\partial n}\left(\mu\frac{\partial k}{\partial n}\right)_w = \left(\mu\frac{\partial k}{\partial n}\right)_1 \Big/ 3\Delta n_1 = \frac{\mu(k_2 - k_1)}{3\Delta n_1 \Delta n_2} \tag{17}$$

with

$$\Delta n_1 = n_1 - n_w, \qquad \Delta n_2 = n_2 - n_1$$

Conservation Equations

The conservation equations used in conjunction with the preceding model are given by Eqs. (5.43–5.45) of Ref. 1. After modeling, these equations can be written as

$$\frac{\partial \bar\rho}{\partial t} + \frac{\partial}{\partial x_j}(\bar\rho \tilde u_j) = 0 \tag{18}$$

$$\frac{\partial}{\partial t}(\bar\rho\tilde u_i) + \frac{\partial}{\partial x_j}(\bar\rho\tilde u_i\tilde u_j) = -\frac{\partial \bar P}{\partial x_i} + \frac{\partial}{\partial x_j}(\bar t_{ij} + \tau_{ij}) \tag{19}$$

$$\frac{\partial}{\partial t}(\bar\rho\tilde E) + \frac{\partial}{\partial x_j}(\bar\rho\tilde u_j\tilde H) = \frac{\partial}{\partial x_j}\left[\left(\frac{\mu}{Pr} + \frac{\mu_t}{Pr_t}\right)\frac{\partial \tilde h}{\partial x_j} + \left(\mu + \frac{\mu_t}{\sigma_k}\right)\frac{\partial k}{\partial x_j} + \tilde u_i(\bar t_{ij} + \tau_{ij})\right] \tag{20}$$

where the Favre-averaged total energy and enthalpy are

$$\tilde E = \tilde e + \tfrac{1}{2}\tilde u_i\tilde u_i + k \tag{21}$$

$$\tilde H = \tilde h + \tfrac{1}{2}\tilde u_i\tilde u_i + k \tag{22}$$

and e and h are the internal energy and enthalpy per unit mass and Pr is the Prandtl number with subscript t designating turbulent; Pr_t is chosen as 0.9.

Numerical Issues

We have used the k–ζ model for calculating a wide range of problems. The following represents some suggestions for smooth implementation in Navier–Stokes solvers. The codes used in this work employ Runge–Kutta time-stepping schemes. Typically, the code is run for about 100 iterations in the laminar mode. To speed up transition to turbulence, δ may be set to zero for several hundred iterations and then reset to its value of 0.1.

Two terms resulted in numerical oscillations in the transient phase. The first is the term that results from the skew-symmetric component of the second-order tensor $\widetilde{\omega_i'' u_j''}$, which is given in term of the derivatives of the turbulent stresses. When convergence is achieved, this term is very small compared to the symmetric part of the tensor and, thus, if desired, can be neglected. The second is the coefficient of β_8. Here again, if one sets $\beta_8 = 0$ for a couple of hundred iterations and then resets it to its value of 2.3, oscillations resulting from this term during the transient phase of integration can be reduced or completely eliminated.

The model acts like k–ε for high turbulent Reynolds numbers and, thus, does not have any sensitivity to freestream boundary conditions. In general, k_∞ is specified from conditions of the experiment. Values of $(\nu_t/\nu)_\infty$ ranging from 10^{-1} to 10^{-6} were employed in the present work without affecting the solution.

Results and Discussion

All cases considered involve flows where separation plays an important role and where Morkovin's assumption is expected to hold. Other calculations are available in Refs. 4–7.

Two-Dimensional Flows

Results are presented here for three different airfoils: RAE 2882, NACA 0012, and NACA 4412. Comparisons were made with the k–ω model, the Johnson and King (JK) model (results taken from Ref. 9), and experiment. The k–ω model is an option in our code and was selected because it is coordinate independent and because it generally performs better than available k–ε models for wall-bounded flows in the presence of mild adverse pressure gradients.[1] It is to be noted that Menter's[10] shear stress model performs extremely well when two-dimensional separated flows are considered. However, the model is coordinate dependent; moreover, it modifies the definition of eddy viscosity and production terms. Because of this, the model is not an option in our code and, thus, no direct comparison with Mentor's model is presented.

A summary of all two-dimensional cases considered together with grids employed is shown in Table 2. Grid studies were conducted but are not included here except, as an illustration, calculations of the RAE 2822 employed the following grids: 321×91, 231×51, and 143×41. The first two grids gave almost identical results. Similar tests were conducted for the other airfoils. The grids indicated in Table 2 give grid-independent solutions. All calculations set the outer boundary at a distance of about 10 chords. It has been determined from the grid analysis that the k–ζ model requires a minimum of approximately five points within $y^+ \le 10$ and an initial $y^+ < 1$. Transition to turbulence was preset in all calculations presented here.

The Navier–Stokes solver employed is a modification of a solver developed by Gaffney et al.[11] It solves the two-dimensional, time-dependent, thin-layer, Reynolds-averaged Navier–Stokes equations with a finite volume formulation. It employs the third-order, biased, flux difference splitting of Roe for the inviscid terms and central differencing for the viscous terms. It is advanced in time using a four-stage Runge–Kutta scheme.

Figures 1 and 2 compare pressure coefficient C_p and skin friction coefficient based on edge conditions, C_{fe}, for case 10 of the RAE 2822. Experimental results are given by Cook et al.[12] No definitive angle of attack or Mach number corrections to account for wall interference effects were given. As a result, flow conditions assumed for this case were those adopted by Rumsey and Vatsa.[13] For this case, shock-induced separation is indicated. Both the present and JK models do a good job predicting pressure distribution and skin friction. The delayed and milder separation indicated by the k–ω model is representative of traditional two-equation models and is a result of the high eddy viscosity predicted by such models.

The next set of experiments involves the NACA 0012 airfoil for two sets of freestream conditions. Unfortunately, skin-friction data are not available. Therefore, comparisons are limited to pressure data taken from Ref. 14. Figure 3 shows results for an angle of attack α of 8.34 deg and a freestream Mach number $M_\infty = 0.55$. As is seen from Fig. 3, all models predict pressure distribution well. Figure 4 compares predictions with experiment for $\alpha = 2.26$ deg and $M_\infty = 0.799$. In this case, both the present and the JK models give good agreement with experiment, whereas the k–ω model indicates delayed transition.

The final case considered is the NACA 4412, and the data are taken from Ref. 15. For this case $M_\infty = 0.2$ and $\alpha = 13.87$ deg, and separation is a result of large-pressure gradient. No skin-friction

Table 2 Airfoil cases considered

Airfoil	Mach number	Re	Angle of attack, deg	Grid
RAE 2822 (case 10)	0.75	6.2×10^6	2.72	231×61
NACA 0012	0.55	9.0×10^6	8.34	287×71
NACA 0012	0.80	9.0×10^6	2.26	237×51
NACA 4412	0.20	1.5×10^6	13.87	237×91

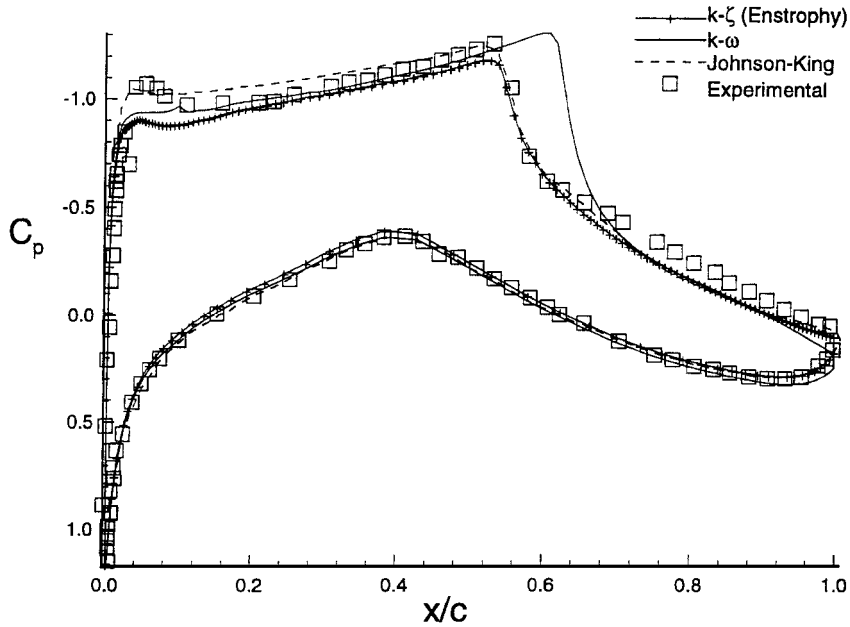

Fig. 1 RAE 2822 (case 10) pressure coefficient.

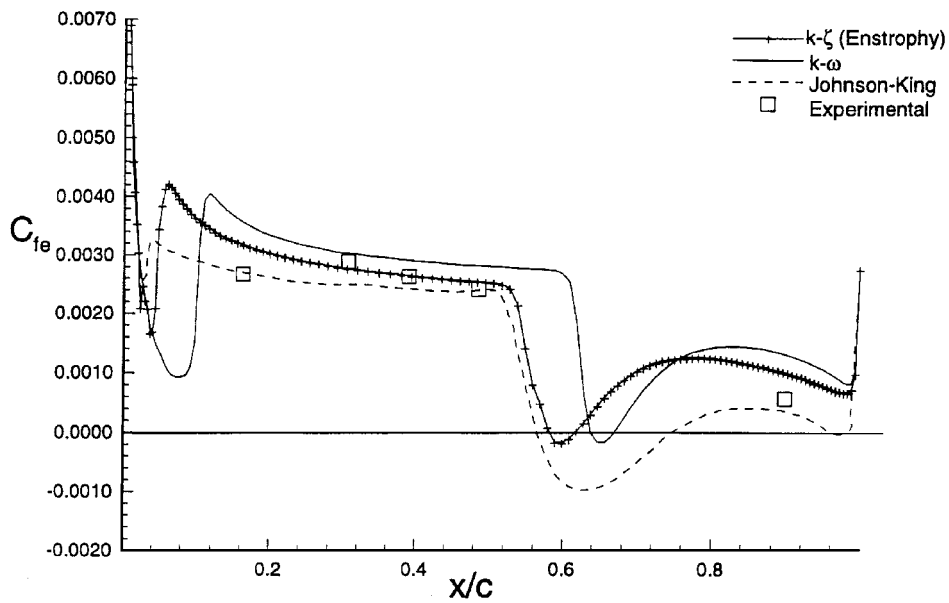

Fig. 2 RAE 2822 (case 10) skin-friction coefficient.

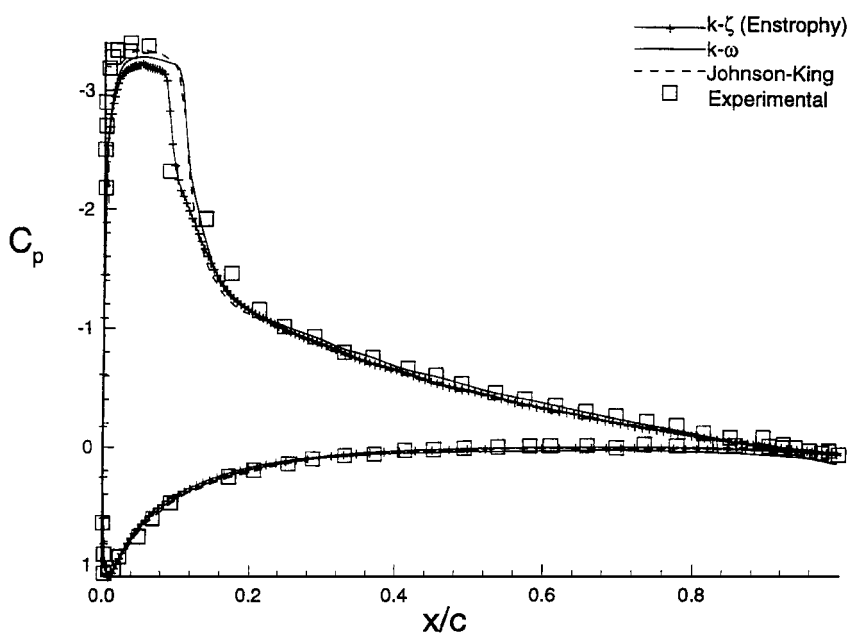

Fig. 3 NACA 0012 pressure coefficient: $M_\infty = 0.55$ and $\alpha = 8.34$ deg.

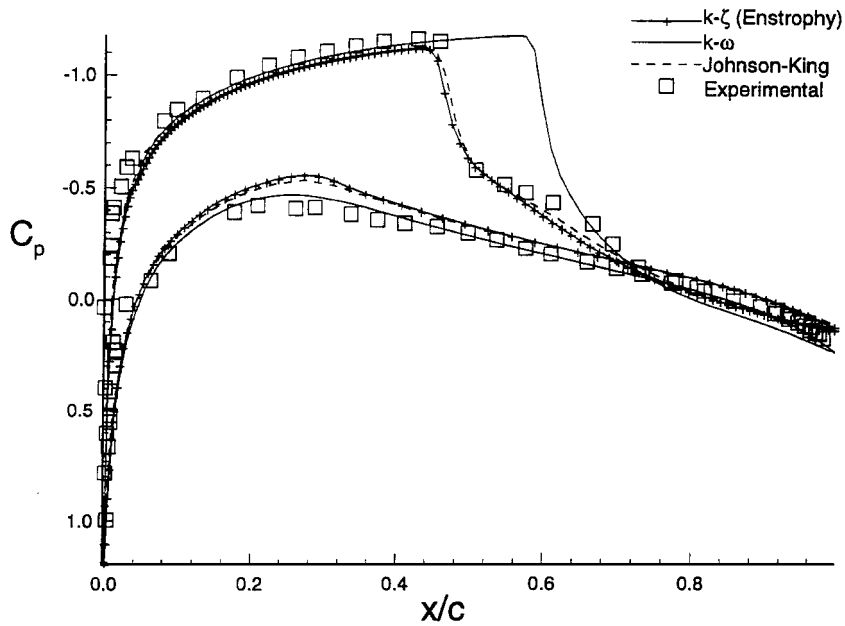

Fig. 4 NACA 0012 pressure coefficient: M_∞ = 0.799 and α = 2.26 deg.

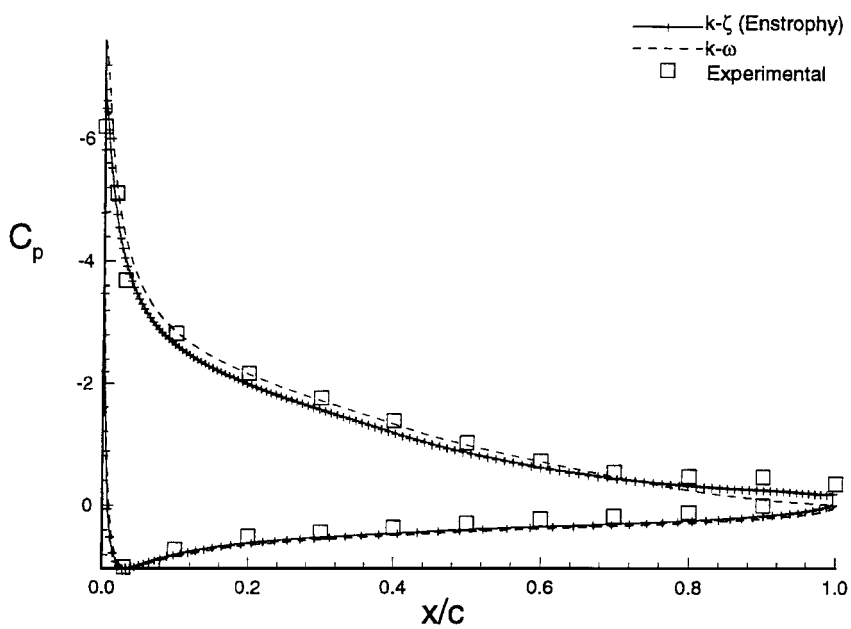

Fig. 5 NACA 4412 pressure coefficient.

data are available. However, Coles and Wadcock[15] indicate that separation took place between $x/c = 0.75$–0.80, suggesting that the flow was not steady. Figure 5 shows that both the present and the k–ω models predict the pressure distribution quite well. Skin-friction calculations in Fig. 6 show that the k–ζ model predicts separation at $x/c = 0.81$, in good agreement with experiment, whereas k–ω predicts delayed and milder separation. Figure 7 compares the mean velocity profiles for a variety of x/c locations. Again, predictions of the current theory are more consistent with experiment.

Three-Dimensional Flows

The three-dimensional flow considered is that over a cylinder/offset flare juncture shown in Fig. 8. It consists of a sting-supported cylinder forming a juncture with a conical flare whose half angle is 20 deg. Details of the geometry are shown in Fig. 9.

The primary reasons for selecting this configuration are the steady flow and the availability of surface pressure and skin-friction measurements.[16] Moreover, the skin-friction measurement was essentially nonintrusive. Both the pressure distribution and skin friction were provided at three different planes: $\theta = 0$, 90, and 180 deg. The angle θ is measured with respect to the cylinder axis with $\theta = 0$ and 180 deg, referring to the upper and lower symmetry planes. The wall is assumed to be adiabatic with an adiabatic wall temperature of 262 K. The incoming Mach number is 2.89, and the angle of attack is zero.

The experiment was a subject of detailed investigation by Gaitonde et al.[17] and Edwards and Chandra[18] using a variety of one- and two-equation models. Following the approach employed in Refs. 17 and 18, the problem was split into two problems: an axisymmetric problem over the cylinder, followed by a three-dimensional problem over the cylinder/flare juncture. The starting profile for the three-dimensional calculations was selected at the point where cylinder calculations matched measured pressure distribution over total pressure P/P_t, skin friction, and boundary-layer thickness. The initial profile was placed at about 10 cm from the juncture. This corresponds to about 10 initial boundary-layer thicknesses $\delta \approx 1.1$ cm. Based on the experience of Refs. 17 and 18, a grid consisting of $87 \times 99 \times 99$ points was employed. The grid generator was the one used in Refs. 17 and 18. The code employed

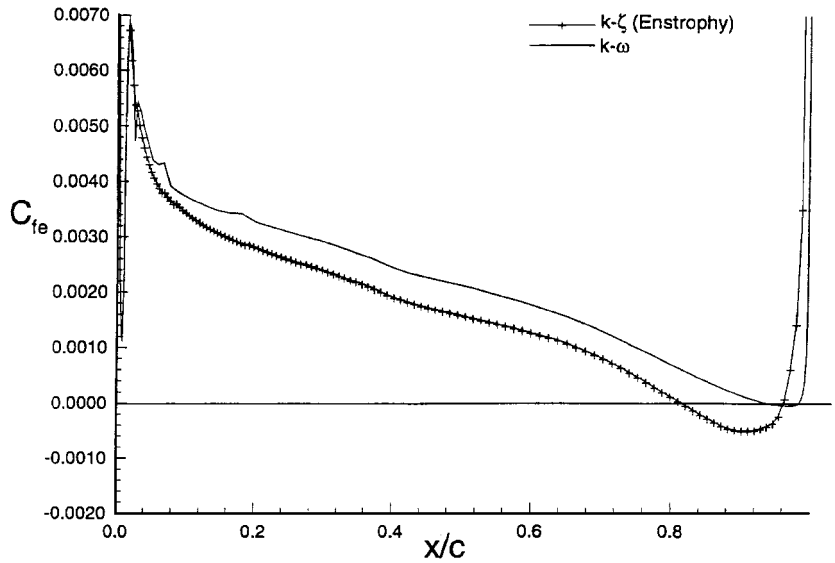

Fig. 6 NACA 4412 skin-friction coefficient.

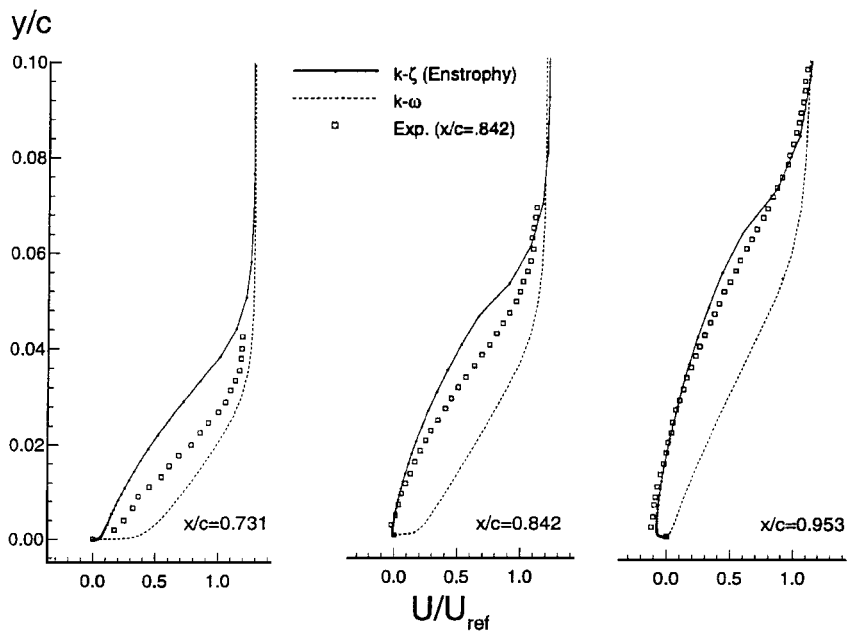

Fig. 7 NACA 4412 velocity profiles.

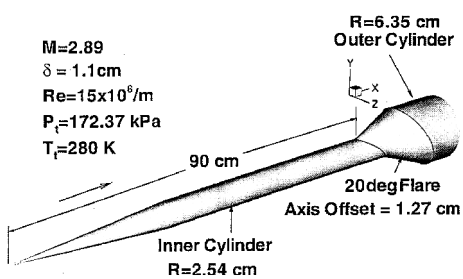

Fig. 8 Geometry of cylinder/offset-flare juncture.

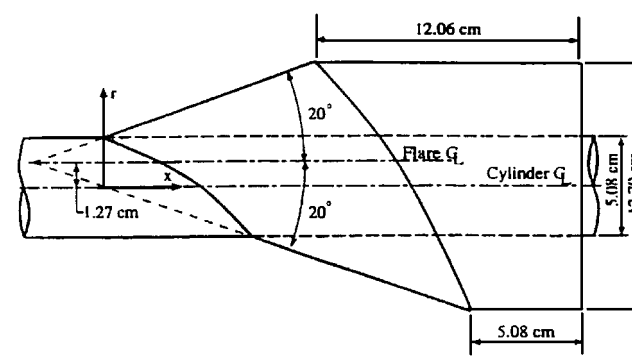

Fig. 9 Schematic of three-dimensional flare.

is an adaptation of the code developed by Baurle et al.[19] It is a central difference code with scaler damping. Time stepping is achieved by employing a four-stage Runge–Kutta scheme. Initial y^+ is 0.3. Regarding boundary conditions, extrapolation was employed at the outer boundary, a no slip at the adiabatic wall, and symmetry at the upper and lower symmetry planes.

Comparisons are made with experiment and the k–ε results of Ref. 17 provided by Gaitonde. For clarity of presentation, comparison is limited to the k–ε model because it gave best overall agreement with experiment. Figures 10–12 show the pressure ratio for $\theta = 0$-, 90-, and 180-deg planes, respectively. The pressure ratio is equal to the surface pressure over the freestream stagnation pressure. For the $\theta = 0$-deg plane, both models accurately predict the initial pressure rise upstream of the juncture. This indicates that, for this plane, both models are accurately predicting the extent of the separation bubble. Downstream of the juncture, the k–ζ model shows a pressure rise that is in closer agreement with the experimental data. However, both models predict asymptotic pressure region accurately. For the $\theta = 90$-deg plane, both models again do a good job of predicting the

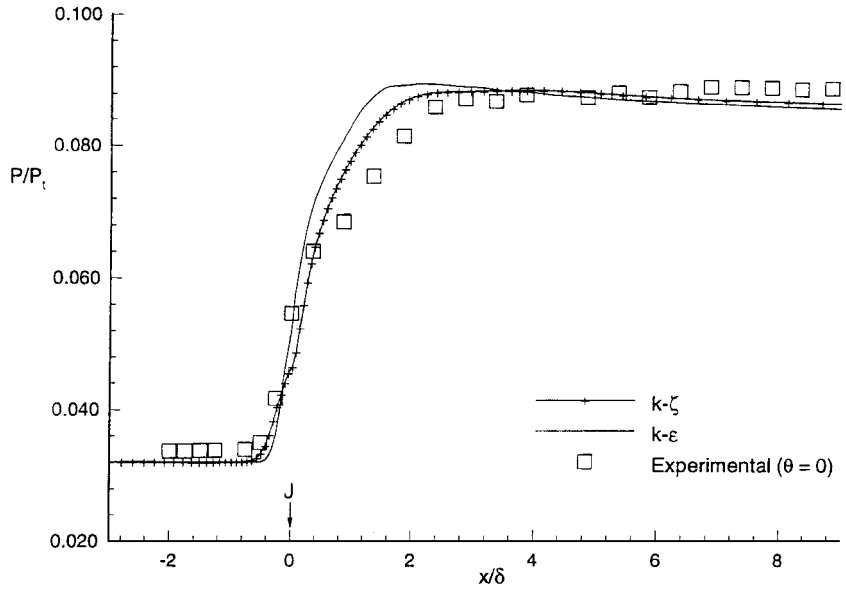

Fig. 10 Streamwise pressure coefficient: θ = 0 deg.

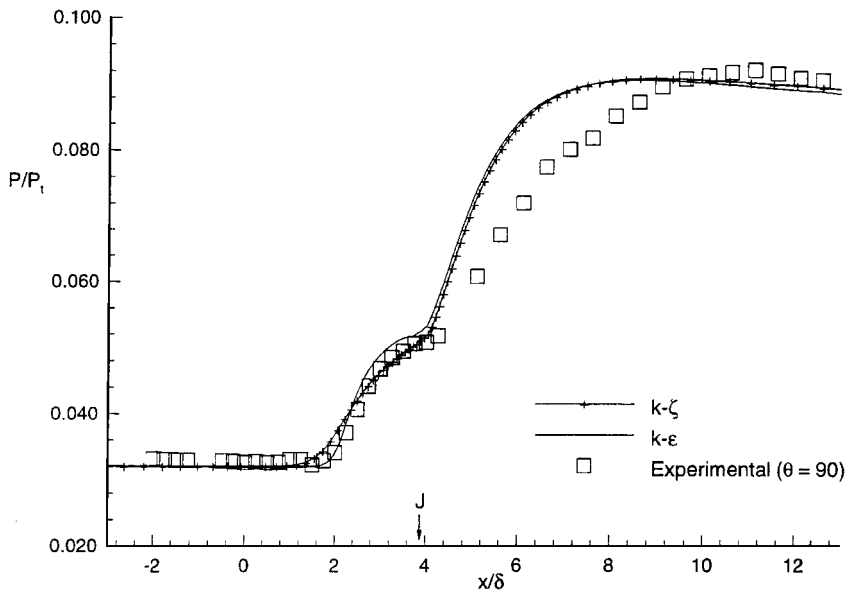

Fig. 11 Streamwise pressure coefficient: θ = 90 deg.

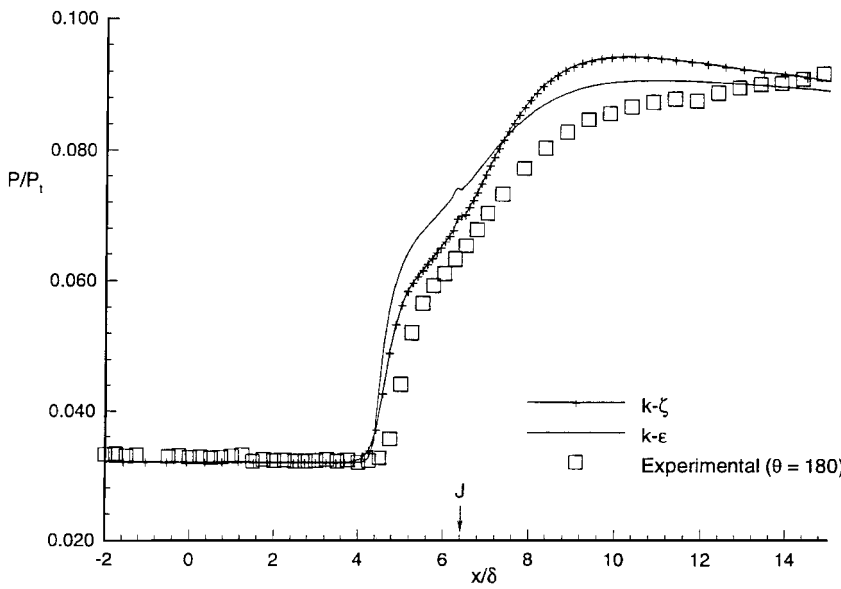

Fig. 12 Streamwise pressure coefficient: θ = 180 deg.

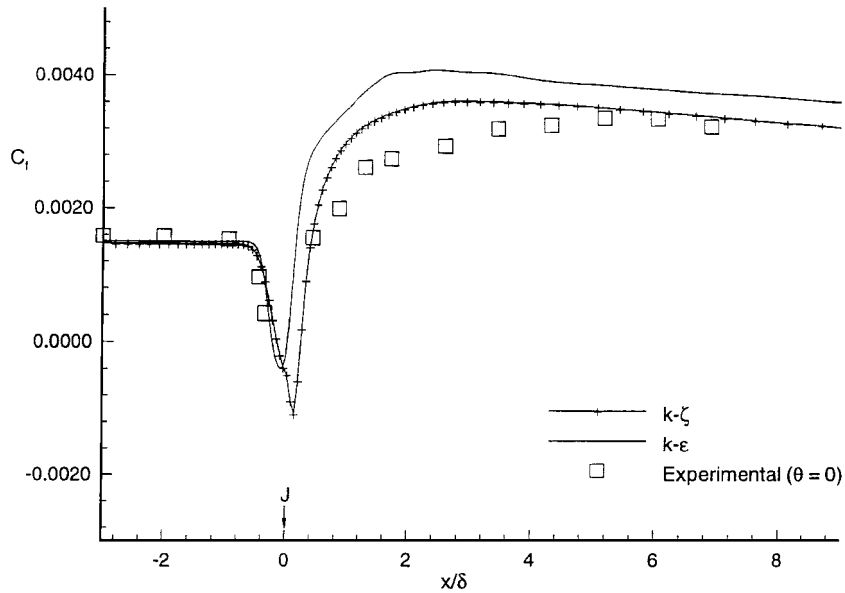

Fig. 13 Skin-friction coefficient: θ = 0 deg.

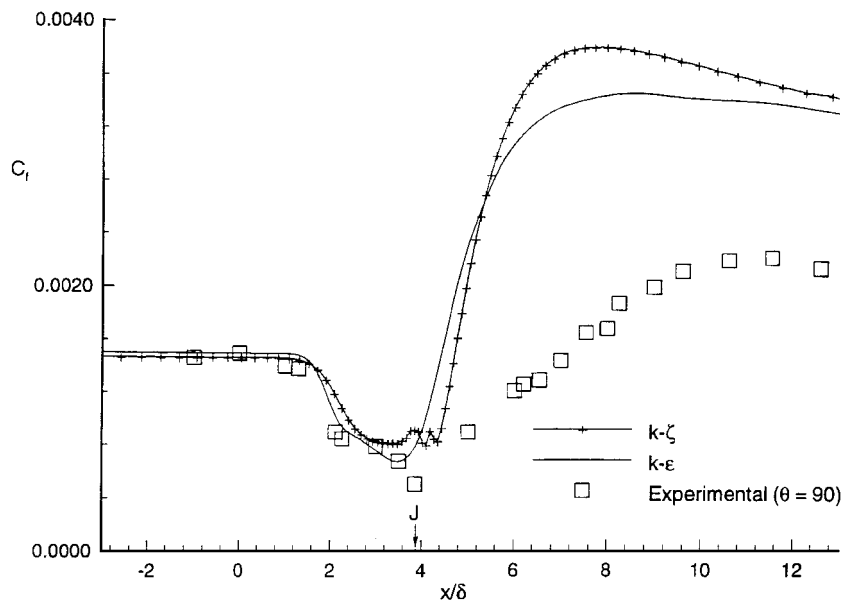

Fig. 14 Skin-friction coefficient: θ = 90 deg.

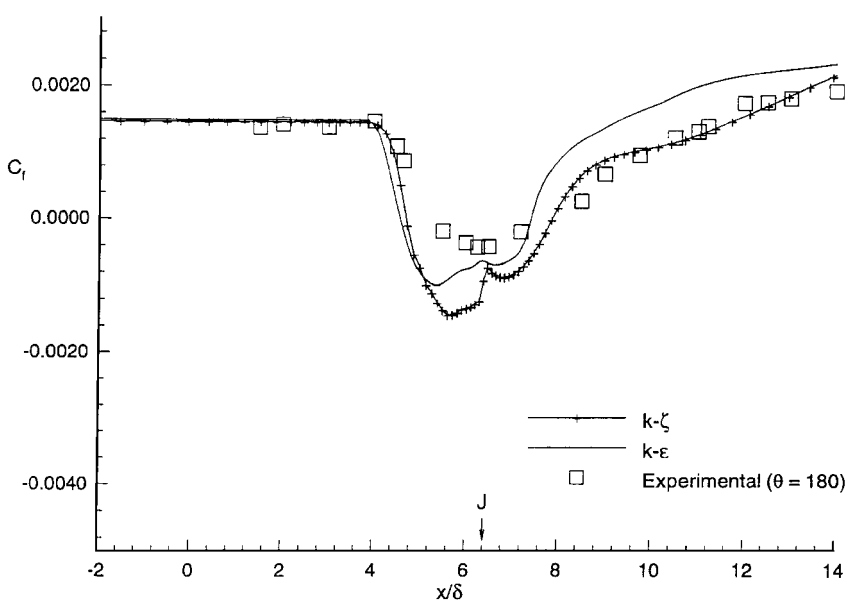

Fig. 15 Skin-friction coefficient: θ = 180 deg.

initial pressure rise aft of the juncture, and both models then overpredict pressure ratio, but they both return to acceptable levels in the downstream region. The results for $\theta = 180$ deg show that the k–ζ model does a slightly better job of predicting the pressure ratio upstream of the juncture. Aft of the juncture, it shows a slightly higher peak; however, it returns to an acceptable level in the downstream region. It is observed from Figs. 10–12 that upstream influence is minimum at the $\theta = 0$-deg plane, where low cross velocities exist. It increases until the $\theta = 90$-deg plane is reached, at which point the upstream influence is maximum. This value then remains relatively constant until the bottom symmetry plane is reached.

Figures 13–15 show the skin-friction coefficient C_f (made dimensionless using freestream properties) for the $\theta = 0$-, 90-, and 180-deg planes, respectively. For the $\theta = 0$-deg plane, the k–ζ model does a better job predicting C_f downstream of the juncture. The k–ε model overpredicts the asymptotic value for the skin friction. The C_f for the $\theta = 90$-deg plane show that both models mimic each other closely and significantly overpredict the skin-friction data in the downstream region. Discussions with James Brown, one of the authors of Ref. 16, indicated that the data for the $\theta = 90$ deg are in error on the flare region downstream of the junction, i.e., point J in Fig. 14. Therefore, a meaningful discussion of the performance of the model for this particular case is not possible. It should be noted that, although the skin-friction data for the region indicated are in error, the pressure data for the $\theta = 90$-deg plane is accurate (private communication, James Brown, NASA Ames Research Center, 1997). Figure 15 shows the skin-friction comparison for the $\theta = 180$-deg plane. The k–ζ model slightly overpredicts the separated region; however, it does an excellent job downstream of the juncture.

As may be seen from the results, the three-dimensional version of the k–ζ model narrows the gap between theory and experiment especially when predicting gradient quantities such as skin friction. The accurate skin-friction measurements of Ref. 16 can be confirmed by other means for attached flows. The same cannot be said for separated regions (private communication, James Brown). Because of this, it is difficult to assess discrepancies between theory and experiment in such regions.

Concluding Remarks

The present investigation completes the formulation of a two-equation k–ζ model that is tensorially consistent, Galilean, and coordinate invariant, as well as free of wall and damping functions. It is shown that the model predicts two- and three-dimensional flow rather well. This work further indicates that it is possible to develop a two-equation turbulence model that is capable of predicting two- and three-dimensional separated flows without sacrificing performance for free shear flows. The key to this success is the inclusion in the ζ equation of the fine-structure correlations that play a major role near turbulent/nonturbulent interfaces.

Appendix: Modeled Equations

The final form of the modeled k–ζ equations can be written as

$$\frac{\partial}{\partial t}(\bar{\rho}k) + \frac{\partial}{\partial x_j}(\bar{\rho}\tilde{u}_j k) = \frac{\partial}{\partial x_j}\left[\left(\frac{\mu}{3} + \frac{\mu_t}{\sigma_k}\right)\frac{\partial k}{\partial x_j}\right] + \tau_{ij}\frac{\partial \tilde{u}_i}{\partial x_j} - \frac{1}{C_k}\frac{\mu_t}{\bar{\rho}^2}\frac{\partial \bar{\rho}}{\partial x_i}\frac{\partial \bar{P}}{\partial x_i} - C_1\frac{\bar{\rho}k}{\tau_\rho} - \mu\zeta \tag{A1}$$

$$\frac{\partial}{\partial t}(\bar{\rho}\zeta) + \frac{\partial}{\partial x_j}(\bar{\rho}\tilde{u}_j \zeta) = \frac{\partial}{\partial x_j}\left[\left(\mu + \frac{\mu_t}{\sigma_\zeta}\right)\frac{\partial \zeta}{\partial x_j}\right] + \frac{\mu_t}{\sigma_r}\frac{\partial \Omega_i}{\partial x_j}\left(\frac{\partial \Omega_i}{\partial x_j} + \frac{\partial \Omega_j}{\partial x_i}\right) - \varepsilon_{mij}\frac{\partial \Omega_i}{\partial x_j}\left[\frac{\partial}{\partial x_\ell}(u_m'' u_\ell'') - \frac{\partial k}{\partial x_m}\right] + \left(\alpha_3 b_{ij} + \frac{1}{3}\delta_{ij}\right)\bar{\rho}\zeta\tilde{s}_{ij} - \frac{\beta_4 \zeta \tau_{ij}\Omega_i\Omega_j}{k\Omega} - \frac{\beta_5}{R_k + \delta}\bar{\rho}\zeta^{\frac{3}{2}} - \frac{2\beta_6\tau_{ij}\nu_t}{k\nu}\Omega\Omega_i\Omega_j + \frac{\beta_7\bar{\rho}\zeta}{\Omega^2}\Omega_i\Omega_j\tilde{s}_{ij} + 2\beta_8\varepsilon_{ilm}\left(\frac{\tau_{ij}}{k}\right)\frac{\partial k}{\partial x_l}\frac{\partial \zeta}{\partial x_m} \times \frac{\Omega_j}{(\bar{s}^2 + \Omega^2/2)} + \max[P_\zeta, 0] - 2\bar{\rho}\zeta\tilde{s}_{ii} - C_{\zeta 1}\frac{\mu_t \zeta\Omega}{\tau_\rho k} \tag{A2}$$

where P_ζ is defined in Eq. (14).

Acknowledgments

The work was supported in part by NASA Grant NAG-1-244. The authors would like to express their appreciation to D. Gaitonde, U.S. Air Force Research Laboratory, for providing the results of his k–ε calculations for the cylinder/flare juncture problem; J. R. Edwards, North Carolina State University, for many helpful discussion regarding grid employed in cylinder/flare juncture problem; and James Brown, NASA Ames Research Center, for discussion relevant to the experimental results. Further, the authors would like to acknowledge the North Carolina Supercomputing Center for use of their facilities.

References

[1]Wilcox, D. C., "Turbulence Modeling for CFD," DCW Industries, Inc., La Cañada, CA, 1993.

[2]Morse, A. P., "Axisymmetric Free Shear Flows with and Without Swirl," Ph.D. Dissertation, Dept. of Mechanical Engineering, Imperial College of Science and Technology, Univ. of London, London, May 1980.

[3]Robinson, D. F., Harris, J. E., and Hassan, H. A., "Unified Turbulence Closure Model for Axisymmetric and Planar Free Shear Slows," *AIAA Journal*, Vol. 33, No. 12, 1995, pp. 2324–2331.

[4]Robinson, D. F., and Hassan, H. A., "A Two-Equation Turbulence Closure Model for Wall Bounded and Free Shear Layers," AIAA Paper 96-2057, June 1996.

[5]Alexopoulos, G. A., and Hassan, H. A., "A k–ζ (Enstrophy) Compressible Turbulence Model for Mixing Layers and Wall Bounded Flows," AIAA Paper 96-2039, June 1996.

[6]Robinson, D. F., and Hassan, H. A., "Modeling of Separated Turbulent Flows," AIAA Paper 97-0207, Jan. 1997.

[7]Robinson, D. F., and Hassan, H. A., "Modeling Turbulence Without Damping Functions Using k–ζ Model," AIAA Paper 97-2312, June 1997.

[8]Morkovin, M., "Effects of Compressibility on Turbulent Flows," *Mecanique de le Turbulence*, edited by A. Favre, Gordon and Breach, New York, 1964, pp. 367–380.

[9]Rumsey, C. L., and Anderson, W. K., "Parametric Study of Grid Size, Time Step, and Turbulence Modeling on Navier–Stokes Computations over Airfoils," CP-437, Vol. 1, AGARD, May 1988, pp. 5.1–5.19.

[10]Menter, F. R., "Two-Equation Eddy Viscosity Turbulence Models for Engineering Applications," *AIAA Journal*, Vol. 32, No. 11, 1994, pp. 1299–1310.

[11]Gaffney, R. L., Salas, M. D., and Hassan, H. A., "An Abbreviated Reynolds Stress Turbulence Model for Airfoil Flows," AIAA Paper 90-1468, June 1990.

[12]Cook, P., McDonald, M., and Firmin, M., "Airfoil RAE 2822—Pressure Distribution and Boundary Layer Measurements," AR-138, AGARD, May 1979.

[13]Rumsey, C. L., and Vatsa, V. N., "A Comparison of the Predictive Capabilities of Several Turbulence Models Using Upwind and Central-Difference Computer Codes," AIAA Paper 93-0192, Jan. 1993.

[14]Harris, C., "Two-Dimensional Aerodynamic Characteristics of the NASA 0012 Airfoil in the Langley 8-Foot Transonic Pressure Tunnel," NASA TM-81927, 1981.

[15]Coles, D., and Wadcock, A. J., "Flying Hot Wire Study of Flow Past an NACA 4412 Airfoil at Maximum Lift," *AIAA Journal*, Vol. 17, No. 4, 1979, pp. 321–328.

[16]Wideman, J. K., Brown, J. L., Miles, J. B., and Özcan, O., "Surface Documentation of a Three-Dimensional Supersonic, Shock-Wave/Boundary Layer Interaction," NASA TM-108824, June 1994; also "Skin-Friction Measurements in Three-Dimensional, Supersonic Shock-Wave/Boundary-Layer Interaction," *AIAA Journal*, Vol. 33, No. 5, 1995, pp. 805–811.

[17]Gaitonde, D., Shang, J. S., and Edwards, J. R., "The Computed Structure of a 3-D Turbulent Interaction Caused by a Cylinder/Offset Flare Juncture," AIAA Paper 95-0230, Jan. 1995.

[18]Edwards, J. R., and Chandra, S., "Comparison of Eddy Viscosity-Transport Turbulence Models for Three-Dimensional, Shock-Separated Flowfields," *AIAA Journal*, Vol. 34, No. 4, 1996, pp. 756–763.

[19]Baurle, R. A., Alexopoulos, G. A., and Hassan, H. A., "Analysis of Supersonic Combustors with Swept Ram Injectors," *Journal of Propulsion and Power*, Vol. 13, No. 2, 1997, pp. 327, 328.

G. M. Faeth
Editor-in-Chief